Patterns of Spontaneous Initiation and Termination of Reentry in a Loop of Cardiac Tissue: Introducing A Threshold Model

VCU project to study temporal patterns of cardiac arrhythmia occurrences

Ventricular arrhythmia is a leading cause of cardiac arrest and sudden death. Clinical observations and implantable cardioverter defibrillators have accumulated a substantial amount of data on the occurrences of ventricular arrhythmia in patients [1, 36, 38, 39, 53, 59-61]. Temporal patterns of initiations and terminations of tachycardia tend to exhibit substantial variations across different time scales and their occurrences do not correlate decisively with medication, exertion, stress, lifestyles and similar factors. Tachycardia events are not random; they show circadian patterns [36, 60] and also tend to occur in clusters. However, the detection times between consecutive events and clusters are spread out over time [38, 53, 59], making it difficult to understand their causes and make predictions about their occurrences. Unlike the circadian patterns, these clusterings or their patterns of occurrences are not affected by the long-term administration of antiarrhythmic drugs [59]. In spite of the abundant data in existence, the reasons for the ways in which these patterns occur are not well-understood.

Many factors, ranging from internal cardiac mechanisms to external chance events play significant roles in shaping the electrocardiogram (ECG) recordings and the implantable defibrillator data. Separating all of the possible contributions is a formidable task, but understanding the influences of various factors and the extent to which each plays a role may have important consequences for the diagnosis and treatment of tachyarrhythmias. A number of prior studies using special preparations of animal cell cultures establish that complex, spontaneously generated patterns may occur without some of the features peculiar to the heart (e.g. the 3-dimensional geometry or biological features such as valves, different tissue layers and types, etc.) [3, 25, 35, 45]. These studies also indicate (both theoretically and experimentally) that causes external to the heart, whether random or deterministic, are not always necessary for the occurrence of irregular behavior. A different class of studies that involve interactive self-oscillatory sources also establish the capability of basic cardiac mechanisms to generate complex rhythms without considering the whole heart [23, 28, 44].

From these and similar studies it may be concluded that changes in the basic internal cardiac mechanisms can play a significant role in generating and sustaining arrhythmias. To clarify the role of these basic internal mechanisms at a fundamental level, we focus on the unidirectional reentrant circulation of action potentials in a loop of ventricular tissue. Because of their pervasiveness and the relative simplicity of their nature, reentrant loops have received a great deal of attention [4, 8, 11, 14-16, 20, 26, 30, 42, 45, 49-51]. Studying *spontaneous initiation and termination of reentry* (SITR) patterns in the loop context is considerably simpler than in the whole heart and can offer potentially useful insights into the clinically observed patterns of arrhythmia. In the construction of a workable model, a certain level of abstraction bridges over physiological complexities that do not play a central role in the long-term evolution of temporal patterns.

We consider a model that combines the traditional discrete loop with a pacer to form an

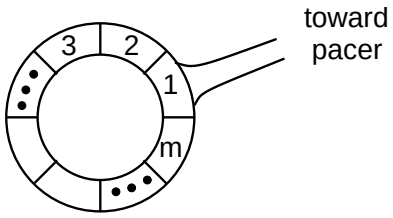

Figure 1: Schematic diagram of a loop joined to the rest of the heart by a single conducting pathway.

interactive system. Fundamental thresholds are dynamically integrated so they can either trigger reentry or inhibit it. Although a relatively simple mechanism, this composite system has two important features: It is an essential component of a well-known cardiac anomaly; and it is capable of generating complex initiation and termination patterns.

In a series of case-studies we show that the loop-pacer mechanism may be responsible for irregularities in onset and termination of reentry beyond such pervasive factors as tissue heterogeneity, the geometry of the heart and other physiological and non-physiological factors. Even without such complexities, the SITR patterns generated by the loop-pacer system can be complex; i.e. they contain many regular features yet their evolution over time is difficult to predict. We trace this complexity to the interaction of a threshold with the bistability of the reentrant circulation and in some cases, also to the inherent discontinuity of phase resetting interactions between the loop and the pacer. Bistability is an inherent physiological characteristic that may be attributed to non-uniformities in the restitution of *action potential duration* (APD); this feature emerges prominently when *conduction velocity* (CV) is properly matched with APD. When this happens (e.g. when the length of the loop is within a certain range) the SITR patterns become considerably more complex and unpredictable.

1 The threshold model.

In this section we briefly describe the loop-pacer threshold model.

1.1 The loop.

Consider a loop of cardiac tissue consisting of cells that conduct action potentials and assume that a single conducting pathway connects the loop to the rest of the heart. Let the physical length of the loop be denoted by L measured in centimeters. Divide the loop into m sets or aggregates of cells, each of which may be called a *cell aggregate* or for brevity, just a "cell." The cell aggregate that is connected to the only pathway out of the loop is also the gateway through which pulses enter the loop or exit it; we label it Cell 1; see Figure 1. This cell is adjacent not only to Cell 2, but also to Cell m at its other end.

For each integer i between 1 and m, label the length of the i-th Cell ΔL_i. These cell aggregates' lengths are not necessarily equal but of course, they add up to L. Since each cell aggregate must have at least one cardiac cell in it, ΔL_i has a natural lower bound, namely the nominal length of a single cardiac cell (about 0.01 cm). The closer all ΔL_i are to this lower bound, the greater is the number m of cell aggregates in a loop of fixed length L; for a 12 cm loop with cells of length 0.01 cm, the number of cells is 1200. While for discrete modeling it is not necessary to pick m that large, it needs to be large enough (hence each cell aggregate small enough) that the conduction velocity from one end of an aggregate to the other can be taken to be approximately constant. This assumption is essential if the restitution of *conduction time* (CT) is defined in terms of the restitution of CV, as we do later on.

We assume that all the cardiac cells within a given aggregate are identical. If all cells in the *entire loop* have identical physiological characteristics then we may also let cell aggregates all have equal lengths. In such a case, the loop is said to be "homogeneous." Otherwise the loop is "heterogeneous."

To initiate unidirectional circulation, it is necessary that a unidirectional block (UB) exist somewhere in the loop; for simplicity, we place it in Cell 1, the gateway to the loop; see Figure 1. Thus Cell 1 is able to activate Cell 2 but not Cell m. For our simulations, we use a simplified version of the time window that is defined by a cut-off value DI^* for the *diastolic interval* (DI); i.e. conduction is blocked in any cell whose recovery period DI is not greater than DI^*. Such a minimum value is used in [26] as a termination mechanism for explaining the experimental results of [20]; also see [19].

1.2 Restitution functions.

We use the term "restitution" generally for relations that give a particular quantity, e.g. action potential duration or conduction time as a function of the diastolic interval. The DI (usually measured in milliseconds, ms) is the rest or recovery period for the cell which essentially starts with the end of the refractory period and ends when the cell is activated again.

1.2.1 APD restitution.

In its most basic form, the action potential duration or APD is the length of time (usually measured in milliseconds, ms) that a cell is active after excitation. For our purposes, we may think of APD as a cell's *effective refractory period* (ERP) during which no excitations, even strong ones, can elicit new action potentials. The restitution of APD which can be experimentally measured or derived from ionic models, is the most extensively studied of restitution relations [2, 4-8, 10, 11, 21, 24, 26, 29, 32, 33, 43, 47, 49, 51, 54-58]. Any APD restitution function, whether experimentally measured or analytically derived can be used in this model. For numerical simulations we use an APD restitution function that is fitted to the experimental data by Koller, et al [33] where APD values were recorded in two types of patients, those with and those without structural heart disease

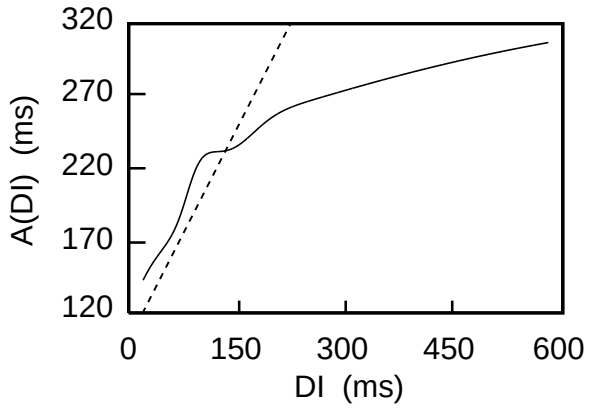

Figure 2: Graph of the APD restitution curve given by (1). The dashed line has slope 1 and is included for reference.

(SHD). The following is a possible fit to their averaged data displayed in Figure 1 in [33] for SHD patients:

$$A(DI) = a_1 - a_2 e^{-\sigma_1 DI} - a_3 e^{-\sigma_2 (DI-\tau_1)} - a_4 e^{-\sigma_3 (DI-\tau_2)^2} + \frac{a_5 (DI-\tau_3)}{(DI-\tau_3)^2 + a_6} \tag{1}$$

with parameter values

a_1	a_2	a_3	a_4	a_5	a_6	σ_1	σ_2	σ_3	τ_1	τ_2	τ_3
350	157	8	20	1700	1200	0.0021	0.025	0.0004	80	136	82

A graph of this function is shown in Figure 2.

1.2.2 CT restitution.

Each cell conducts an action potential through it in a finite amount of time. This time interval, usually measured in milliseconds, is referred to as the conduction time (CT) [4, 26, 51]. Experimentally measured CT restitution functions are not as readily available for human hearts as the APD restitution functions; however, they may be readily derived from CV restitution functions through the relation

$$C(DI) = \frac{\Delta L}{V(DI)} \tag{2}$$

where C and V are, respectively, the CT and the CV restitution functions. This derivation is valid if as mentioned earlier, V is essentially constant over the length of each cell (or cell aggregate) and thus no spatial dependence is required in V.

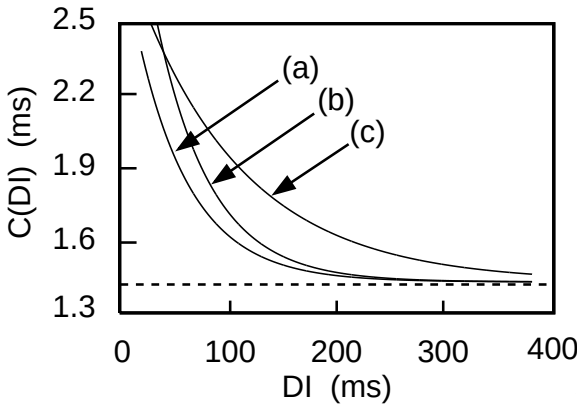

Figure 3: Graph of the CT restitution curves given by (3) for several choices of parameters. For each curve, $\Delta L = 0.1$ and $c = 0.07$. (a) $d = 1$ and $\omega = 0.02$; (b) $d = 1.5$ and $\omega = 0.02$; and (c) $d = 1$ and $\omega = 0.01$.

For some discussions of CV restitution functions see [2, 7, 8, 11, 12, 14-16, 20, 22, 54, 55, 57]. For our simulations we use the following expression

$$C(DI) = \frac{\Delta L}{c}[1 + de^{-\omega DI}], \quad DI > 0 \tag{3}$$

with parameter values:

ΔL	c	d	ω
0.1 cm	0.07 cm/ms	1	0.02 ms^{-1}

These numbers are obtained using (2) and a reasonable fit to the human-rescaled, guinea pig data for CV from [22, 55]. By changing these parameters we achieve conduction slow-downs in different ways, as shown in Figure 3.

1.3 The interactive pacer.

In the absence of reentry a pacer (the sinus node or an ectopic focus) drives the ventricles. If reentry is initiated and interrupted then the pacer and the loop cycle out of phase and it is necessary to carefully model their interaction. For this purpose we define two rhythms, or clocks: The pacer's rhythm which has a prescribed beat pattern, and the system's rhythm which is reset when reentry initiates or terminates.

Starting from a given reference point in time, we denote the time of occurrence of the k-th pacer beat by β_k and the time of occurrence of the n-th system beat by ρ_n. If no reentrant beats occur

then these two quantities have the same index and are equal. Otherwise, we define the *first* pacer pulse that reaches Cell 1 in beat n as the *least* integer k_n such that

$$\beta_{k_n} > \rho_n + \delta_n. \tag{4}$$

The variable delay term δ_n here represents a *time lag* that results from the blocking of the pacer by the reentrant wave propagating in the opposite direction (toward the pacer). δ_n may generally depend on several factors including the location of the loop in the heart and the surrounding pathologies, a possible conduction slow-down in the permitted direction in the proximity of a UB site, the number and nature of pathways that connect the loop to the rest of the heart and the dynamic state of the loop.

If the loop is not in reentry, then δ_n may take the minimum value DI^* since Cell 1 must have at least that much rest time after its ERP before it can be reactivated. If the loop was in reentry in beat $n-1$ then a wavefront would propagate from the site of the loop and enter the main body of the heart where it would annihilate any incoming waves from the pacer. To model additional delays in the arrival of the next pulse from the pacer that may be caused by this interaction, we use a value δ larger than DI^*. Thus a simple definition for δ_n is the following:

$$\delta_n = \begin{cases} \delta, & \text{if pulse } n-1 \text{ was reentrant} \\ DI^*, & \text{otherwise} \end{cases}, \ \delta > DI^*.$$

High frequency reentrant waves typically disassociate a slow pacer such as the sinus node. This situation is modeled here by choosing a sufficiently large value of the pacer delay parameter δ so as to inhibit the pacer from interfering with the reentrant circulation. Small values for δ, which promote pacer interference, may be feasible in certain circumstances, e.g. when there are pathways from the pacer's site to the site of the loop that are protected from the fast reentrant waves by pathologies.

Using a single parameter δ to account for all the circumstances that determine the time lag δ_n is clearly an over-simplification; but even with this minimalist definition, some of the simulations below indicate that the scalar parameter δ may play a significant role in the evolution of SITR by affecting the frequency of stray pulses that can enter the loop while it is in reentry.

A different mechanism of two competing oscillators has been studied in models of parasystole, where a permanent ectopic rhythm coexists with the sinus or another rhythm [23, 28, 44]. Studies of these models have shown that even under restricted conditions complex patterns may arise that are highly sensitive to parameter changes, including any alterations in the refractory period of cells. As might be expected, a mathematical relation with a discontinuity is responsible for the complexity of temporal patterns; see [23, 44].

1.4 Modes and thresholds.

We distinguish between two different propagation modes for the loop-pacer system: The *reentry mode* where an action potential continually circulates in the loop and the *paced mode* where the

action potential in the loop comes from the pacer. The system's mode in each beat is determined by two threshold relations. To define these thresholds, first we define the following quantities:

> The *pacer's lag* in beat n is $PL_n = \beta_{k_n} - \rho_n$; and:
>
> The *projected DI* of Cell i in Beat n or $PDI_{i,n}$ is the time that it takes a pulse to return to Cell i, minus APD of Cell i.

Note that while PL_n always exceeds DI^* by (4), the quantity $PDI_{i,n}$ can be negative (which happens should the pulse arrive before the end of the ERP).

We now define the *circulation threshold TC* (or *head-tail* or *conduction block threshold*) and the *pacer threshold TP* (or *phase resetting threshold*) as follows:

$$\begin{array}{l}\text{TC holds for Cell } i \text{ when} \quad PDI_{i,n} > DI^*; \\ \text{TP holds when} \quad PL_n > PDI_{1,n}.\end{array}$$

We say that Beat n is in reentry mode if TP holds and TC holds, at least for Cell 1; i.e. if

$$PL_n > PDI_{1,n} > DI^*.$$

Otherwise, Beat n is in paced mode.

2 SITR patterns.

In this section we present the results of numerical simulations of our threshold model along with some analytical observations. Due to the large number of different types of behavior that can occur by changing one or more of the many variables involved, providing a comprehensive list of essentially different patterns is not feasible here. We therefore present our main results in the form of a few model case-studies and for additional results we refer the interested reader to our web site: *www.people.vcu.edu/~hsedagha/SITR*.

Each case-study below consists of one or more "runs," i.e. sets of iterations of the propagation equations. Each run is based on a fixed set of parameter values and we call each iteration in a given run a "beat". For each run we need to specify m initial DI values $DI_{i,0}$. This specification of DI values is a technical representation of the occurrence of a premature stimulation in our model.

2.1 Mode sequences.

The following conventions facilitate the presentation of results in this section:

> If in a loop consisting of m cells a reentrant pulse is blocked at Cell j in a particular beat, then we define the *reentry value* of that beat as the ratio $(j-1)/m$; this ratio will be abbreviated as $[\,j]$.

If a reentrant pulse completes a turn around the loop then the reentry value is 1.

If a reentrant pulse is blocked in Cell j after t complete turns around the loop then the reentry value is $t[\,j]$.

If a beat occurs in the paced mode (i.e. one of the thresholds TC or TP fails) then we assign it the value -1. t consecutive beats in paced mode appear as $-t$.

If the pattern is locked in the reentry mode, we use the symbol ∞; if it is locked in the paced mode, we use $-\infty$.

Adding up consecutive reentry mode beats and consecutive paced mode beats gives a sequence of numbers consisting of integers whose sign tell us the mode of system in various sets of beats. Examples of mode sequences and more details on them are found in the case-studies below.

2.2 Bistability and thresholds.

We call the loop-pacer system *bistable* if there are two or more coexisting stable DI configurations or state vectors, each of which can be reached from a particular region of the m-dimensional state space. If there are more than two distinct, coexisting stable states then the system is *multistable*.

Bistability may be attributed to the non-concavity of the APD restitution function [51]. The function (1) whose graph has bumps and twists is also non-concave. Proper CT restitution parameters are required to realize bistability; i.e. the CT and APD restitution parameters must be properly matched. Because the length L of the loop affects the conduction time through it, bistability may emerge or fade as L is changed with other CT parameters fixed [51].

A bistable regime can affect SITR patterns by causing the violation of the circulation threshold TC without any changes in the APD or CT parameters, or any changes in the pacing rate. This situation occurs if the bistable regime satisfies the following *threshold bistability* condition:

T-bistability: There are two distinct stable states in the reentry mode: In one state the DI values cross the value DI^* and cause the failure of the circulation threshold TC at some cell within the loop, but in the other state the DI^* value is never reached.

An example of T-bistability is shown Figure 6 below; other examples of T-bistability occur in the next section (Case-study 1). The m-dimensional state space of a T-bistable system is partitioned into two regions or basins of attraction. As a SITR pattern evolves with the motion of the DI state vector, mode changes occur if the state vector crosses over into the basin of attraction of a different stable regime.

2.3 Case-study 1: T-bistable reentry.

In this section we establish that T-bistability lends a measure of unpredictability to SITR patterns that is not due to phase resetting disruptions by the pacer (i.e. TP failures). For instance, comparing the mode sequences in Runs 1.2, 1.4 and 1.6 below we see that the initial few bursts of fast, reentrant beats provide no obvious clues about the eventual modes that the patterns lock into.

Consider a homogeneous loop with the APD and CT restitutions given by (1) and (3). We also set the length L and other parameters as:

L	m	DI^*	δ	B_0
12.5 cm	125	15.3 ms	120 ms	320 ms

where B_0 is the fixed cycle length of the pacer; it is chosen small in this case-study to facilitate reinitiations of reentry. The value of δ is set high enough to inhibit pacer interference (TP never fails). The following table summarizes the results of simulations; it is followed by a series of observations and elaborations.

Run No.	$DI_{i,0},\ i = 1, \ldots 125$	SITR pattern mode sequence
1.1	200 ms	$\{-2, 2, -2, 2, \ldots\}$
1.2	100 ms	$\{-2, 4, -2, 32[73], -2, \infty\}$
1.3	80 ms	$\{-1, \infty\}$
1.4	70 ms	$\{4, -2, 14, -2, 4, -2, 22[49], -\infty\}$
1.5	60 ms	$\{\infty\}$
1.6	50 ms	$\{11, -2, 4, -2, 27[57], -2, \infty\}$

(i) In Run 1.1 the SITR pattern immediately locks into a regular form of 2 paced beats followed by 2 reentrant beats. In Runs 1.2, 1.3, 1.5 and 1.6 the SITR pattern locks into the reentry mode. In Run 1.4 the paced mode is locked into. Note that the only thing that is changing from one run to the next is the initial DI values.

(ii) In Runs 1.2, 1.3, 1.5 and 1.6 the DI values in the sustained or locked reentry modes converge to a fixed number and the eventual values of the fundamental parameters are

DI	APD	cycle length CL = APD+DI
59.4 ms	173.6 ms	233 ms

The fixed, limiting DI value 59.4 represents a stable *convergent state*. This equilibrium DI is locally stable (attracting) because using the restitution functions (1) and (3) we compute [4, 26]

$$A'(59.4) + C'(59.4) = 0.90 < 1.$$

(iii) In Runs 1.2, 1.4 and 1.6 all the spontaneously terminated reentry bursts have oscillating (quasiperiodic) DI. Thus APD and CL also oscillate. The oscillatory state is stable and eventually

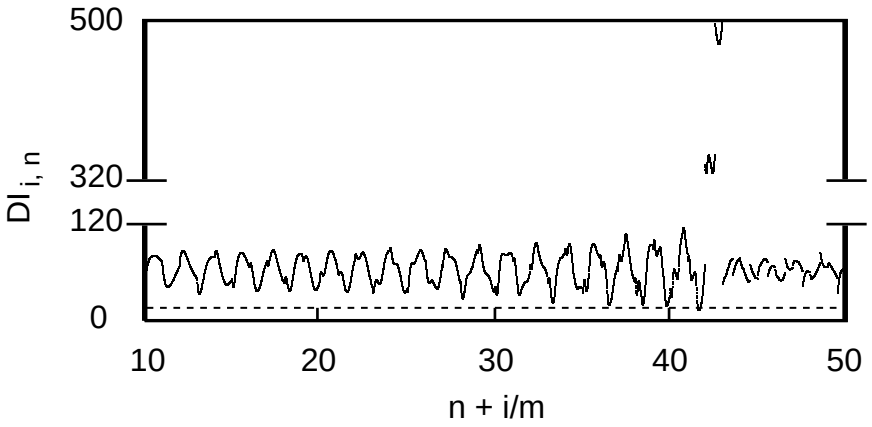

Figure 4: Results of Run 1.2, showing variation of DI in Beats 10 through 50. The dashed line corresponds to $DI^* = 15.3$. Amplification of oscillations in DI leads to termination of reentry in Beat 41, Cell 73 because $DI_{73,41} < DI^*$.

crosses $DI^* = 15.3$ ms. Hence there is T-bistability (the oscillatory one and the convergent one) which causes the mode changes in each run as well as changes in SITR patterns from run to run.

For example, in Run 1.2 the 2nd initiation of reentry (the 32-beat burst) starts with the DI state-vector in the basin of attraction of an oscillatory state which expands enough for the DI values to cross DI^* (TC fails); see Figure 4. This terminates the second reentry burst at Cell 73 in the 41st beat. This is the same type of termination mechanism as that in [19, 20, 26]; this type of oscillations in DI are also seen in [57] where they are related to the T wave alternans in ECG recordings; also see [35] in this regard. With the 3rd initiation of reentry, the DI state-vector falls in the basin of attraction of the convergent state which then effectively "traps" the DI trajectory and locks the SITR pattern into the reentry mode (here then, simplicity of behavior is not a good thing).

(iv) Examination of the simulation data for Run 1.4 shows a recurrent failing of TC in Cell 1 after the last burst of 23 reentrant beats. For all sufficiently large values of n,

$PDI_{1,n}$	PL_n	$DI_{1,n}$	$APD_{1,n}$	CL_n
-18.95	96.6	96.6	223.4	320

The circulation threshold TC fails repeatedly (pulses blocked at Cell 1) since the projected DI value is negative. The number 96.6 is the equilibrium DI for the paced mode if pacing period $B_0 = 320$. The equilibrium DI happens to be stable. To see this, note that in the absence of reentry the paced mode is governed by the one-dimensional difference equation

$$DI_{1,n} = F(DI_{1,n-1}) = B_0 - A(DI_{1,n-1})$$

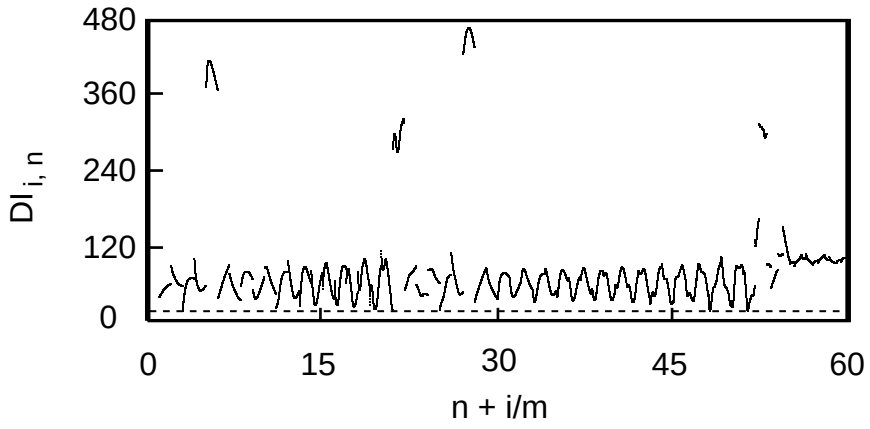

Figure 5: Results of Run 1.4, showing variation of DI in Beats 1 through 60. The dashed line corresponds to $DI^* = 15.3$.

with $F'(96.6) = -A'(96.6) = -0.901$; i.e. $|F'(96.6)| < 1$. Why the transition to the stable paced equilibrium occurs in this run and not others is unclear. Figure 5 shows the changes in DI values in this run.

(v) In Run 1.5, the given initial DI values put the state vector in the basin of attraction of the convergent state of the system. This is evidently not the case in Run 1.6 with even shorter DI. In Run 1.6, as in Run 1.4, the initial mode is oscillating-DI reentry.

(vi) The regular pattern (a cycle of period 4) in Run 1.1 continues indefinitely. The following table lists the values of the fundamental variables for a few beats:

Beat n	$DI_{1,n}$	$APD_{1,n} = A(DI_{1,n-1})$	$APD_{1,n} + DI_{1,n} = CL_n$	$\beta_{k_n} - \rho_n$
96	87.73	169.18	256.91	250.27
97	269.68	212.86	482.54	269.68
98	50.44	269.56	320	50.44
99	54.02	166.53	220.55	153.47
100	87.73	169.18	256.91	250.27

Comparing the 2nd and 5th columns of the above table shows that beats 96, 99 and 100 are not initiated by the pacer; thus they are reentrant.

2.4 Case-study 2: Non-T-bistable reentry.

We now consider some longer loops than in Case-study 1 for comparison. In these loops bistability is present but does not satisfy the T-bistability condition. A smaller variety of different SITR

patterns are obtained (with all other system parameters having the same values as in Case-study 1). We consider two different lengths:

$L = 13$ cm ($m = 130$) where stable oscillating states exist all of which fail TC, but the convergent mode is absent since the DI fixed point of about 62.5 ms is unstable [4, 26]

$$A'(62.5) + C'(62.5) = 1.013 > 1.$$

$L = 14$ cm ($m = 140$) where all of the stable oscillating states (there is at least one) satisfy TC but the convergent mode is again absent for the same reason as above:

$$A'(68) + C'(68) = 1.253 > 1.$$

To save space let us abbreviate repetitions or locked mode patterns with bars:

$$\overline{k, -j} = k, -j, k, -j, \ldots \tag{5}$$

The following table summarizes the results of simulations; it is followed by a series of observations and elaborations.

Run No.	$DI_{i,0}$	$L = 13$ cm	$L = 14$ cm
2.1	200 ms	$\{\overline{-2, 2}\}$	$\{-2, 2, -2, \infty\}$
2.2	100 ms	$\{-2, 4, -2, 12[60], \overline{-2, 2}\}$	$\{-2, \infty\}$
2.3	80 ms	$\{\overline{2, -2}\}$	$\{-1, 1, -2, 2, -2, \infty\}$
2.4	70 ms	$\{12, -2, 10[79], -2, 17[79], \overline{-2, 5[79]}\}$	$\{12, -2, 2, -2, \infty\}$
2.5	60 ms	$\{56, \overline{-2, 2}\}$	$\{-1, 10, -2, 9, -2, \infty\}$
2.6	50 ms	$\{3, -2, 4, -2, 12[60], \overline{-2, 2}\}$	$\{-\infty\}$

(i) The SITR patterns for the 14 cm loop are expected to lock into the reentry mode since the stable states do not fail TC to cause terminations. The exception is Run 2.6 where possibly owing to the greater length of the loop, a pulse from the pacer has time to activate Cell 1 and block the premature simulation from reentering the loop (threshold TP fails). It is not clear why reentry does not re-initiate as in Run 2.5.

(ii) In the case of the 13 cm loop the repeated terminations can be attributed to the fact that the stable states all fail TC; thus the patterns cannot lock into the reentry mode.

(iii) For both of these loops, the eventual form of the SITR pattern is more predictable than the T-bistable loop of Case-study 1. On the other hand, the transient bursts of fast beats still seem difficult to predict.

2.5 Case-study 3: Additional patterns with a fixed pacing rate.

Run 3.1: *More bistability.* This run presents a complex SITR pattern that locks into a long cycle of several initiations and terminations. Make the following changes to parameters in Run 1.2:

d	B_0
1.3	315 ms

Note that the increase in d from 1 to 1.3 in this run causes a slight elevation of the CT restitution curve (i.e., a conduction slow-down).

(i) In this run, after a transient period of spontaneous initiations and terminations, a long 62-beat pattern emerges that is repeated; i.e. the SITR pattern locks into a 62-beat cycle containing several bursts of fast reentrant beats. The mode sequence for this run is as follows, with the pattern between starred numbers repeating:

$$\{-2, 8[81], -1, [35], -2, 4, -2, 7[24], -1, [18], -2, 8[18],^* -1, [12], -2, 7[12], -1, [12], -2,$$
$$10[49], -2, 5[49], -2, 4, -2, 7[22], -1, [19], -2, 7[19],^* -1, [12], -2, 7[12], -1, [12], -2, \ldots\}$$

(ii) The DI equilibrium of approximately 64 ms is unstable in this run since

$$A'(64) + C'(64) = 1.073 > 1.$$

This instability is caused by the greater value of d and results in the absence of the convergent state. Nevertheless, there is T-bistability where one of the stable oscillating states does not fail TC but another oscillating state does. In the first oscillatory state, DI values come very close to DI^*; see Figure 6. This proximity increases the sensitivity to transient effects of mode changes and makes locking into the reentry mode an improbable event.

Run 3.2: Functional heterogeneity. In this run we highlight the occurrence of conduction block in the paced mode and the resulting spatial functional heterogeneity that such a block creates in the loop. We only change the pacing period in Run 3.1 to $B_0 = 310$ ms.

(i) The mode sequence in this case is:

$$\left\{-2, 7[16], -2, 7[46], -3, 7[46], -2, 7[46], -3, 4, -2, 8[93], -2, 7, \overline{-2, 2}\right\}.$$

Thus the SITR pattern locks into a 4-beat cycle in this case.

(ii) Of particular interest are the two pairs of non-reentrant beats 21,22 and 42,43 within the 3-beat paced stretches in the mode sequence. Since in Beat 20 the reentrant pulse had been blocked in Cell 46, it follows that cells 46-125 did not fire an action potential in that beat and thus remained at rest. This creates a 2-tier DI profile in Beat 21: cells 1-45 have a shorter DI than cells 46-125. Now Beat 21 itself is blocked in Cell 3 by failing TC, even though it is initiated by the pacer

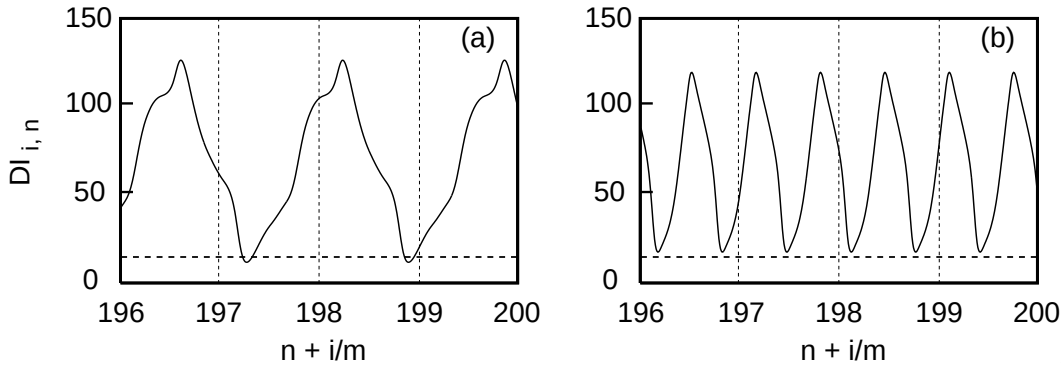

Figure 6: Results of Run 3.1 if $DI^* = 0$ instead of 15.3. (a) If $DI_{i,0} = 67$ for all i, the graph crosses the dashed horizontal line $DI = 15.3$. Thus, if we had set $DI^* = 15.3$, reentry would not be sustained. (b) $DI_{i,0} = 66$ for all i. Reentry is sustained with quasi-periodic variation of DI.

(hence it does not appear explicitly in the mode sequence). This in turn creates a 3-tier functional heterogeneity in the DI values in Beat 22:

$$DI_{1,22} = 164.31,\ DI_{2,22} = 168.41$$
$$304.70 \leq DI_{i,22} \leq 321.98,\ i = 3, \ldots, 45$$
$$453.81 \leq DI_{i,22} \leq 490.95,\ i = 46, \ldots, 125.$$

(iii) A similar 3-tier, heterogeneous profile exists for Beats 42 and 43 with conduction block occurring in Cell 7 in Beat 42 in the paced mode. See Figure 7.

2.6 Case-study 4: Pacer interactions.

In Case-studies 1-3 we see that the convergent reentry pattern is "sticky" i.e. once this pattern is attained, reentry does not self-terminate by the circulation mechanism in the loop. However, interaction of the pacer with the loop can lead to termination in some cases either (a) immediately, by the pacer's injection of a properly timed stray pulse into the loop or (b) eventually, by changing the convergent pattern to a terminating oscillatory one in a T-bistable case.

Each interference with the reentrant circulation by the pacer is flagged here through a failure of the pacer threshold TP. These interferences often do not lead to terminations, especially if they occur in a long loop or when conduction velocity is small so that the conducting pathway out of the loop has a greater chance of being inactive between reentrant pulses. But the failure of TP is possible even in small homogeneous loops by sufficiently reducing the value of the delay parameter δ.

Run 4.1: All parameters are as in Run 1.5 (hence there is T-bistability) except that now

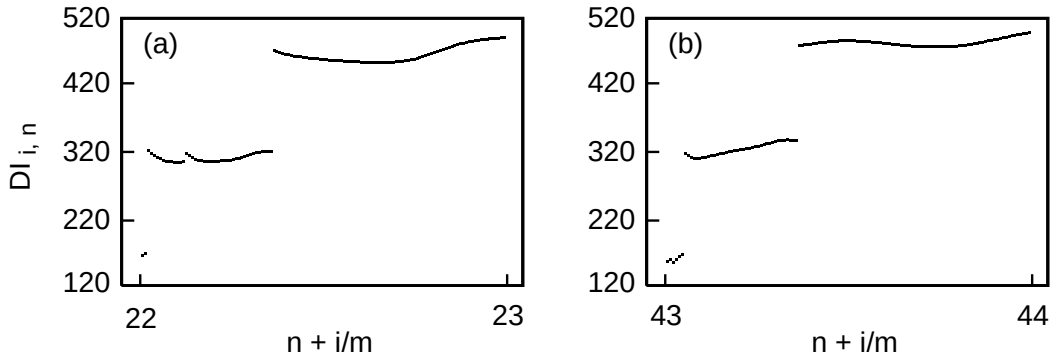

Figure 7: Results of Run 3.2 showing variation of DI in (a) Beat 22 and (b) Beat 43.

δ	B_0
45 ms	800 ms

We have set the pacing period at the nominal sinus length to eliminate the effects of fast pacing.
(i) The mode sequence for this run is:

$$\{40, -1, 15, -\infty\}.$$

(ii) Reentry is initiated with Beat 1 by a premature stimulation, and the DI values begin to approach the limiting value 59.4 ms as in Run 1.5. However, TP fails in Beat 41; a stray pulse from the pacer enters the loop and changes the reentry DI pattern from the convergent type to an oscillating one; see Figure 8.

The oscillating DI pattern crosses the DI^* threshold (TC fails) in Beat 55 and reentry terminates in this beat.

Run 4.2: All parameters are as in Run 4.1 except that $\delta = 46$. *Reentry terminates by a stray pulse.* Also the reentry pattern changes due to T-bistability.
(i) The mode sequence for this run is:

$$\{64, -1, 78, -1, 31, -\infty\}.$$

(ii) TP fails in Beats 65, 144 and 175. The stable convergent pattern is disturbed but does not change after Beat 65; the convergent pattern changes to oscillatory after Beat 144.
(iii) The TP failure in Beat 175 leads to conduction block at Cell 2 in the next beat; since this block occurs in paced mode, it does not appear in the mode sequence. The pacer's stray pulse reenters the loop, as in Beats 66 and 145, but this time it is quickly blocked. Reentry terminates with Beat 176 and does not re-initiate.

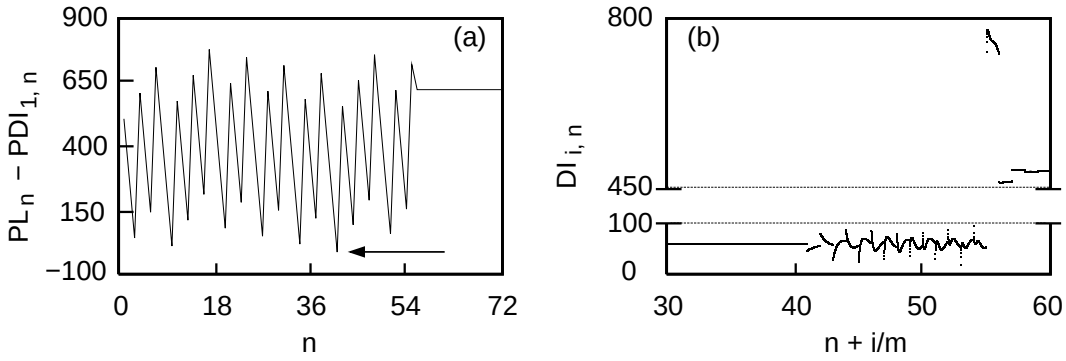

Figure 8: Results of Run 4.1. (a) $PL_n - PDI_{1,n}$ for $n = 1, 2, \ldots 100$. The negative value in Beat 41 (indicated by the arrow) corresponds to termination of reentry due to failure of TP. (b) DI values in Beats 30 through 60.

2.7 Case-study 5: Variable-period pacing.

Knowing what types of SITR patterns are generated with fixed-period pacing does not go far enough in providing insights into the nature and causes of cardiac rhythm anomalies. If reentry is not sustained indefinitely then the DI profile of the loop (i.e. its DI state vector) varies with the changing frequency of a variable-rate pacer, a situation that can lead to significant changes in the SITR patterns. Remarkably, *changing the length, or the period, of the pacer's cycle of oscillations can affect a SITR pattern substantially* (even when leaving all other parameters fixed, including variations of the pacer's oscillation amplitude). To study this and similar situations, in this section we vary the period of the pacer's cycle of oscillations in a sinusoidal fashion:

$$B(k) = B_0 + B_1 \cos\left(\frac{2\pi k}{w}\right).$$

This beat pattern may represent an idealization (without random effects) of a single cycle of a complex, multi-pattern stretch of pacer beats.

The number w is the period of a full cycle of variable-rate oscillations, which we refer to as a *full pacing cycle* (FPC). The halfway point of the FPC, or the "bottom of the FPC well" occurs at $k = w/2$; at this point, the pacer oscillates with minimum period (fastest beat rate). On the other hand, when $k = 0$ or $k = w$ the pacer has its largest oscillation period (slowest beat rate).

The number B_1 is the FPC "amplitude" since it modulates the pacer's oscillation period within the FPC. If $B_1 = 0$ then the period is a fixed B_0 as in the preceding case-studies.

Run 5.1 (*FPC period*): In these runs we examine SITR patterns that are generated by changing the FPC period w only. We take a 12 cm loop ($m = 120$) whose APD parameters are as in the previous case-studies. The following parameters are changed relative to Case-study 1:

L	ω	B_0	B_1	$DI_{1,0}$ to $DI_{120,0}$
12 cm	0.018 ms^{-1}	700 ms	420 ms	each 600 ms

The initial DI values are chosen large to prevent the occurrences of reentry by premature stimulations.

(i) The mode sequences of the SITR patterns are listed in the following table for some values of w:

w	SITR pattern mode sequence
500	$\{-265, [2], -4, 6, -2, 2, -2, 2, -2, 2, -2, 2, -2, 2, -200, \ldots\}$
1000	$\{-495, [2], -37, 1[2], -4, 6, -2, 2, -2, 4, -2, \infty\}$
1500	$\{-721, [2], -77, 1[2], -4, 6, -2, 2, -2, 4, -2, 19[17], -2, [17], -2, 14,$
	$-2, 2, -2, 2, -2, 2, -2, 2, -2, 2, -2, 2, -2, 2, -2, 2, -2, 2, -2, 2, -593, \ldots\}$
5000	$\{-2268, [2], -4, 4, -4, 6, -2, 2, -2, 4, -2, 1, -2, 2, -2, 4, -2, 1, -3, 19,$
	$-1, 27[63], -2, 19[63], -1, [63], -2, \infty\}$

(ii) The initial stretches of beats in the paced mode are due to the amount of time that it takes for the pacing period to decrease sufficiently from its starting high of 1120 ms to a level that will initiate reentry in this particular loop.

(iii) For the FPC periods 500 and 1500 SITR patterns eventually lock into the paced mode until the next FPC. If the next FPC has the same formula as the first, then the same pattern repeats. From the mode sequences listed for these two runs it appears that if the pacing period remained small then the pattern $-2, 2$ would be locked in.

(iv) For the FPC periods 1000 and 5000 the SITR patterns eventually lock into the reentry mode which therefore carry over into the next FPC without spontaneous termination.

(v) For the FPC periods 1000 and 1500 there are unusually long stretches of beats in the paced mode (37 and 77 beats, respectively) *within the same FPC but not at either of the slowly paced ends*. It is unclear why these stretches occur for these values of w but not for others.

(vi) Qualitatively, *this 12 cm loop has the same bistable features of the loop in Case-study 1*. With larger w the interval of time that the pacer spends at high beat rates near the bottom of the FPC well is correspondingly longer. Therefore, differences in the SITR patterns are expected; but given the effects of bistability discussed in previous case-studies, forecasting the type of SITR pattern for a given value of w seems to be difficult.

Note: The results in this run are sensitive to numerical errors and may differ when done with different software or different levels of precision.

Run 5.2 (*FPC amplitude*): For the longest FPC period $w = 5000$ in the preceding run, the first reentrant beat is 2269 (at a pacing period close to 300 ms) and well before the FPC bottom value of 2500 (where the pacing rate is 280 ms). In fact, the mode sequence for this run locks into the sustained reentry mode after Beat 2391, still well before 2500. This observation suggests that

when the FPC period w is large, the pacer may not need to beat quite so fast for the reentry to be initiated.

In this run we keep all parameter values, including the initial DI the same as Run 5.1 but decrease the FPC amplitude B_1 to 400 ms; thus the FPC minimum or bottom value is now 300 ms, occurring at $w/2$, the bottom of the FPC well. We note the following:

(i) With this reduction in pacing rate, reentry is not initiated when $w = 500$ or 1000.

(ii) The mode sequence for $w = 1500$ is as follows

$$\{-769, [2], -2, 9[2], -2, 14[10], -2, 21[10], -2, \infty\}.$$

Thus reentry is initiated in this case and the SITR pattern eventually locks into the reentry mode. This is in contrast to Run 5.1 where with the same value of w the pattern locks into the paced mode.

(iii) The current run shares a feature that is common with that for $w = 500$ in Run 5.1; namely *the first reentrant beat occurs several beats past the minimum FPC value* $w/2 = 750$ ms. The responsible mechanism in both cases is the occurrence of oscillations in the paced mode. For this run with $w = 1500$, this feature is highlighted in the following table:

n	$PDI_{1,n}$	PL_n	n	$PDI_{1,n}$	PL_n	n	$PDI_{1,n}$	PL_n
750	-5.56	87.52	757	-6.05	87.24	764	-1.63	92.32
751	-5.62	87.46	758	-5.27	88.09	765	-12.2	81.90
752	-5.54	87.56	759	-6.51	88.92	766	2.870	97.06
753	-5.68	87.43	760	-4.83	88.69	767	-17.1	77.24
754	-5.51	87.64	761	-7.38	86.22	768	10.39	104.8
755	-5.81	87.38	762	-3.82	89.89	769	-22.2	72.55
756	-5.44	87.79	763	-9.05	84.75	770	17.66	112.3

Reentry starts with Beat 770 where $PDI_{1,770} = 17.66 > DI^*$ (TC holds) and $PDI_{1,770} < PL_{770} = 112.3$ (TP holds). It is clear from the table that these values are reached through oscillations of DI in the paced mode. Before Beat 770, the DI values are given by the quantity PL_n that is generated by the pacer. As seen in the table, this quantity oscillates in the paced mode because the one-dimensional difference equation

$$DI_{1,n} = B(n) - A(DI_{1,n-1})$$

that determines the pacer's pulse pattern exhibits oscillating behavior when $B(n)$ becomes sufficiently small. These oscillations in turn affect PDI_n until this quantity exceeds DI^*.

We note that the occurrence of oscillations in the paced mode is not generally sufficient for the initiation of reentry; if these oscillations occur but the amplitudes of the corresponding oscillations that they induce in PDI_n do not put it over the DI^* value, then reentry is not initiated.

2.8 Case-study 6: Slow pacing, heterogeneity and PVC's.

When the pacing period is slow (say, within the nominal sinus range of 800±350 ms) the CT and APD parameters above do not generate significant SITR patterns. Consider for example, the loop of Case-study 1 with a fixed pacing period of 800 ms. If a premature stimulus does initiate reentry, then either the reentry mode is sustained because the convergent stable state is reached or else, the reentry mode is terminated and the paced mode is sustained thereafter. Therefore, the only SITR patterns that we can expect in this case are $\{\infty\}$, $\{-\infty\}$ and $\{n, -\infty\}$. In the absence of premature stimulations, none of these patterns exhibit *re-initiations* of reentry because for the APD restitution that we are using, the paced mode has a globally attracting fixed point with long pacing periods.

In the present case-study we consider a heterogeneous loop consisting of two patches of cells. Patch 1 consists of cells 1 through j and Patch 2 contains cells $j+1$ and beyond where of course, j is a positive integer less than m, the total number of cells. The cells in Patch 1 may have different APD and/or CT restitution parameters than those in Patch 2.

Run 6.1. We fix the APD and CT parameters for Patch 2 to be the same as those used in Case-study 1. Patch 1 APD has the same parameters as Patch 2 except for the following:

a_1	c	B_0
300 ms	0.05 cm/ms	800 ms

Thus APD is reduced (by a shift in the restitution function) in Patch 1; also the cells in this patch conduct more slowly.

(i) With all initial DI set at 100 ms, the following SITR patterns are obtained for various values of j:

$j = 30$	$j = 40$	$j = 50$	$j = 60$
$\{[31], -\infty\}$	$\{57[44], -\infty\}$	$\{8, -1, 3[51], -\infty\}$	$\{\infty\}$

(ii) In the case $j = 50$ the first interruption of reentry in Beat 9 is by failure of TP, i.e. pacer interference. The second interruption, which also results in termination, is due to the blocking of the reentrant pulse (TC fails) at the junction between patches 1 and 2, where there is a rise in the APD value.

(iii) It is notable that for $j = 40$ the pulse was not blocked at a patch junction (Cell 41).

(iv) For $j = 60$ (and larger j) reentry is sustained because of the greater number of slow conducting cells. It is unclear why no pacer interferences occur in this case since with $j = 60$ cells, conduction is slower than with $j = 50$ cells.

Run 6.2. Parameters are as follows (those not listed are the same as in Run 6.1):

L	a_2	B_0	B_1	w	j	δ
13.5 cm	170 ms	800 ms	350 ms	1000	50	140 ms

The new value of a_2 shifts (lowers) the APD in Patch 1 a little more relative to Run 6.1, while the larger number of cells ($m = 135$) increases conduction time in the loop. The pacing parameters define a variable pacing protocol with FPC period of 1000 beats and amplitude 350 about a fixed, nominal sinus trend of 800 ms.

(i) The mode sequence of the SITR pattern starting with all initial DI 600 ms is

$$\{-464, [51], -1, [51], -1, [51], -1, [51], -1, [51], -2, \infty\}.$$

(ii) The mode sequence exhibits a pattern of 5 incomplete reentry initiations followed by a pacer beat (or 2 in one case). Each incomplete reentry start which is blocked at the patch junction, namely Cell 51, corresponds to a short cycle length (about 224 ms) compared to the pacer's period of approximately 460 ms near the middle of the FPC. Hence the pattern of 5 alternating reentry/pacer beats resembles a series of premature ventricular contractions (PVC) in a bigeminal form [37] before reentry finally takes hold for good. It is likely that if the pacer's period did not decrease further in this case then reentry would not take hold.

(iii) We note that if $j = 40$ or fewer, then no reentry is initiated in this run. On the other hand, larger k than 50 sustain reentry more quickly by increasing the percentage of slow cells in the loop.

3 Summary and discussion.

In the preceding sections, we developed an interactive loop-pacer threshold model that is a part of a familiar cardiac anomaly. Using experimentally measured restitution parameters from the existing literature for action potential duration and conduction time, we obtained various conditions and parameter values that would cause irregular patterns of spontaneous initiations and terminations of reentry.

A major cause of unpredictable behavior is threshold bistability, or T-bistability, where one stable regime causes a failure of the circulation threshold TC and another does not. Since this situation makes the initiation and termination of reentry dependent on where in the state space the loop's DI state vector is, and since the nonlinear propagation equations make it difficult to track this state vector, it is quite difficult to forecast the long-term behavior of an evolving SITR pattern for a T-bistable loop. Another potential source of irregular behavior is the interference by the pacer. If reentry occurs, then the pacer and the reentrant circuit are thrown out of phase and the possibility exists of a phase resetting stray pulse interfering unexpectedly with the reentrant circulation.

The case-studies above explore the dynamics of the anomalous loop-pacer system at a deep level. This type of study makes it possible to identify potential sources of unpredictable behavior (e.g. T-bistability) and to determine the likely physical causes in terms of such things as non-uniformities in the APD restitutions, the conduction velocity characteristics and the length of the loop. Further studies of this type may identify additional significant features.

We omitted many features from our discussion here that one might include in an enhanced version of this model. For example, the time window of the UB could be substantially refined as explained above so as to make the occurrence of UB a functional event caused (and affected) by the dynamics of the system. For this it would be necessary to consider bidirectional propagation in the loop whenever the UB is deactivated and discuss possible failures of the UB threshold. Other enhancements to this model might include adding memory and latency to the APD restitution function, and also a systematic approach to heterogeneity. The inclusion of memory is especially important in clarifying the potential dynamic significance of delayed responses. Additional directions in which one may explore the dynamics of the loop-pacer system include consideration of multiple exit/entry points into the loop that can affect reentry, and also a bit of theory to better model the time lag δ_n that influences the loop-pacer interactions.

With some of the above enhancements the SITR patterns may become more complex and less predictable, though it is possible that some of these enhancements (e.g. memory) can have a moderating effect. Understanding the precise mechanisms that generate such complex SITR patterns may in turn offer useful insights into the nature and causes of long-term temporal patterns of tachyarrhythmia occurrences.

REFERENCES

[1] M.I. Anastasiou-Nana, R.L. Menlove, J.N. Nanas and J.L. Anderson, *Changes in spontaneous variability of ventricular ectopic activity as a function of time in patients with chronic arrhythmias*, Circulation, 78 (1988), pp.286-295.

[2] I. Banville and R.A. Gray, *Effects of action potential duration and conduction velocity restitution on alternans and the stability of arrhythmias*, J. Cardiovascular Electrophysiol., 13 (2002), pp.1141-1149.

[3] Bub, G., K. Tateno, A. Shrier and L. Glass, *Spontaneous initiation and termination of complex rhythms in cardiac cell culture*, J. Cardiovascular Electrophysiol., 14 (2003), pp.S229-S236.

[4] J.W. Cain, *Criterion for stable reentry in a ring of cardiac tissue*, J. Math. Biology, 54 (2007) to appear.

[5] J.W. Cain and D.G. Schaeffer, *Two-term asymptotic approximation of a cardiac restitution curve*, SIAM Rev., 48 (2006), pp.537-546.

[6] J.W. Cain, E.G. Tolkacheva, D.G. Schaeffer and D.J. Gauthier, *Rate-dependent propagation of cardiac action potentials in a one-dimensional fiber*, Phys. Rev. E, 70 (2004), 061906.

[7] J-M. Cao, Z. Qu, Y-H. Kim, T-J. Wu, A. Garfinkel, J.N. Weiss, H.S. Karagueuzian and P-S. Chen, *Spatiotemporal heterogeneity in the induction of ventricular fibrillation by rapid pacing: Importance of cardiac restitution properties*, Circ. Research, 84 (1999), pp.1318-1331.

[8] X. Chen, F.H. Fenton and R.A. Gray, *Head-tail interactions in numerical simulations of reentry in a ring of cardiac tissue*, Heart Rhythm, 2 (2005), pp.851-859.

[9] S.S. Cheng, *Partial Difference Equations*, CRC Press, Boca Raton, 2003.

[10] E.M. Cherry and F.H. Fenton, *Suppression of alternans and conduction blocks despite steep APD restitution: Electrotonic, memory, and conduction velocity restitution effects*, Am. J. Physiol. 286 (2004), pp.H2332-H2341.

[11] E. Cytrynbaum and J.P. Keener, *Stability conditions for the traveling pulse: Modifying the restitution hypothesis*, Chaos, 12 (2002), pp.788-799.

[12] R. Derksen, H.V.M. van Rijen, R. Wilders, S. Tasseron, R.N.W. Hauer, W.L.C. Rutten and J.M.T. de Bakker, Tissue discontinuities affect conduction velocity restitution: A mechanism by which structural barriers may promote wave break, Circulation, 108 (2003), pp.882-888.

[14] D.R. Chialvo, D.C. Michaels and J. Jalife, *Supernormal excitability as a mechanism of chaotic dynamics of activation in cardiac purkinje fibers,* Circ. Research, 66 (1990), pp.525-545.

[14] M. Courtemanche, L. Glass and J.P. Keener, *Instabilities of a propagating pulse in a ring of excitable media*, Phys. Rev. Lett., 70 (1993), pp.2182-2185.

[15] M. Courtemanche, J.P. Keener and L. Glass, *A delay equation representation of pulse circulation on a ring in excitable media*, SIAM J. Appl. Math., 56 (1996), pp.119-142.

[16] M. Courtemanche and A. Vinet, *Reentry in excitable media*, in: A. Beuter, L. Glass, M.C. Mackey and M.S. Titcombe (Ed.s), *Nonlinear Dynamics in Physiology and Medicine*, Chapter 7, Springer, New York, 2003.

[17] S.N. Elaydi, *An Introduction to Difference Equations*, (2nd ed) Springer, New York, 1999.

[18] J.J. Fox, E. Bodenschatz and R.F. Gilmour, *Period-doubling instability and memory in cardiac tissue*, Phys. Rev. Lett., 89 (2002), pp.138101(04).

[19] J.J. Fox, R.F. Gilmour and E. Bodenschatz, *Conduction block in one-dimensional heart fibers,* Phys. Rev. Lett., 89 (2002), pp.198101(04).

[20] L.H. Frame and M.B. Simson, *Oscillations of conduction, action potential duration and refractoriness: A mechanism for spontaneous termination of reentrant tachycardias*, Circulation, 78 (1988), pp.2182-2185.

[21] R.F. Gilmour, M.A. Watanabe and N.F. Otani, *Restitution properties and dynamics of reentry*, In: *Cardiac Electrophysiology: From Cell to Bedside*, 3rd ed., W.B. Saunders, London, 1999, pp.378-385.

[22] S.D. Girouard, J.M. Pastore, K.R. Laurita, K.W. Gregory and D.S. Rosenbaum, *Optical mapping in a new guinea pig model of ventricular tachycardia reveals mechanisms for multiple wavelengths in a single reentrant circuit*, Circulation, 93 (1996), pp.603-613.

[23] L. Glass, A.L. Goldberger, M. Courtemanche and A. Shrier, *Nonlinear dynamics, chaos and complex cardiac arrhythmias*, Proc. R. Soc. Lond. A 413 (1987), pp.9-26.

[24] G.M. Hall, S. Bahar and D.J. Gauthier, *Prevalence of rate-dependent behaviors in cardiac muscle*, Phys. Rev. Lett., 82 (1999), pp.2995-2998.

[25] S-M. Hwang, T.Y. Kim and K.J. Lee, *Complex-periodic spiral waves in confluent cardiac cell cultures induced by localized inhomogeneities*, Proc. Nat. Acad. Sci. USA, 102 (2005), pp.10363-10368.

[26] H. Ito and L. Glass, *Theory of reentrant excitation in a ring of cardiac tissue,* Physica D, 56 (1992), pp.84-106.

[27] J.J. Jack, D. Noble and R.W. Tsien, *Electric Current Flow in Excitable Cells*, Clarendon Press, Oxford, 1975.

[28] J. Jalife, C. Antzelevich and G.K. Moe, *The case for modulated parasystole*, Pace, 5 (1982), pp.911-926.

[29] S.S. Kalb, H.M. Dobrovolny, E.G. Tolkacheva, S.F. Idriss, W. Krassowska and D.J. Gauthier, *The restitution portrait: A new method for investigating rate-dependent restitution*, J. Cardiovascular Electrophysiol., 15 (2004), pp.698-709.

[30] J.P. Keener, *Arrhythmias by dimension*, In: *An Introduction to Mathematical Modeling in Physiology, Cell Biology and Immunology*, J. Sneyd (Ed.), pp.57-81, American Mathematical Society, 2002.

[31] V.L. Kocic and G. Ladas, *Global Behavior of Nonlinear Difference Equations of Higher Order with Applications*, Kluwer, Dordrecht, 1993.

[32] M.L. Koller, M.L. Riccio and R.F. Gilmour, Dynamic restitution of action potential duration during electrical alternans and ventricular fibrillation, Am. J. Physiol. 275 (1998), pp.H1635-H1642.

[33] M.L. Koller, S.K.G. Maier, A.R. Gelzer, W.R. Bauer, M. Meesman and R.F. Gilmour, Altered dynamics of action potential restitution and alternans in humans with structural heart disease, Circulation, 112 (2005), pp.1542-1548.

[34] M.E. Krebs, J.M. Szwed, T. Shinn, W.M. Miles and D.P. Zipes, *Short-term rapid ventricular pacing prolongs ventricular refractoriness in patients*, J. Cardiovascular Electrophysiol., 9 (1998), pp.1036-1042.

[35] A.M. Kunysz, A. Shrier and L. Glass, *Bursting behavior during fixed-delay stimulation of spontaneously beating chick heart cell aggregates*, Am. J. Physiol. 273 (1997), pp.C331-C346.

[36] R. Lampert, L. Rosenfeld, W. Batsford, F. Lee and C. McPherson, *Circadian variation of sustained ventricular tachycardia in patients with coronary artery disease and implantable cardioverter defibrillators*, Circulation, 90 (1994), pp.241-247.

[37] C. Lerma, C.F. Lee, L. Glass and A.L. Goldberger, The rule of bigeminy revisited: Analysis in sudden cardiac death syndrome, J. Electrocardiology, 40 (2007), pp.78-88.

[38] L.S. Liebovitch, A.T. Todorov, M. Zochowski, D. Scheurle, L. Colgin, M.A. Wood, K.A. Ellenbogen, J.M. Herre and R.C. Bernstein, *Nonlinear properties of cardiac rhythm abnormalities*, Phys. Rev. E, 59 (1999), pp.3312-3319.

[39] B. Lown, *Sudden cardiac death: The major challenge confronting contemporary cardiology*, Am. J. Cardiol., 43 (1979), pp.313-328.

[40] E.G. Manios, E.M. Kallergis, E.M. Kanoupakis, H.E. Mavrakis, H.K. Mouloudi, N.K. Klapsinos and P.E. Vardas, *Effects of successful cardioversion of persistent atrial fibrillation on right ventricular refractoriness and repolarization*, Europace, 7 (2005), pp.34-39.

[41] R. Mickens, *Difference Equations: Theory and Applications* (2nd ed), CRC Press, Boca Raton, 1991.

[42] G.R. Mines, *On dynamic equilibrium in the heart*, J. Physiol. (London), 46 (1913), pp.349-383.

[43] C.C. Mitchell and D.G. Schaeffer, *A two-current model for the dynamics of cardiac membrane,* Bull. Math. Biology, 65 (2003), pp.767-793.

[44] G.K. Moe, J. Jalife, W.J. Mueller and B. Moe, *A mathematical model of parasystole and its application to clinical arrhythmias*, Circulation, 56 (1977), pp.968-979.

[45] Y. Nagai, H. Gonzalez, A. Shrier and L. Glass, *Paroxysmal starting and stopping of circulating waves in excitable media*, Phys. Rev. Lett., 18 (2000), pp.184248(4).

[46] J.B. Nolasco and R.W. Dahlen, *A graphic method for the study of alternation in cardiac action potentials*, J. Appl. Physiol., 25 (1968), pp.191-196.

[47] N.F. Otani and R.F. Gilmour, *Memory models for the electrical properties of local cardiac systems*, J. Theor. Biol., 187 (1997), pp.409-436.

[48] R. Plonsey and R.C. Barr, *Bioelectricity: A Quantitative Approach (*2nd ed.), Kluwer Academic/Plenum Publ., NY, 2000.

[49] Z. Qu, J.N. Weiss and A. Garfinkel, *Spatiotemporal chaos in a simulated ring of cardiac cells*, Phys. Rev. Lett., 78 (1997), pp.1387-1390.

[50] W. Quan and Y. Rudy, *Unidirectional block and reentry of cardiac excitation: A model study*, Circ. Research, 66 (1990), pp.367-382.

[51] H. Sedaghat, C.M. Kent and M.A. Wood, *Criteria for the convergence, oscillation and bistability of pulse circulation in a ring of excitable media*, SIAM J. Appl. Math., 66 (2005), pp.573-590.

[52] H. Sedaghat, *Nonlinear Difference Equations: Theory with Applications to Social Science Models*, Kluwer Academic, Dordrecht, 2003.

[53] K.M. Stein, J.S. Borer, C. Hochreiter, and P. Kligfield, Fractal clustering of ventricular ectopy and sudden death in mitral regurgitation, J. Electrocardiol., (suppl) 25 (1992), pp.178-181.

[54] M.D. Stubna, R.H. Rand and R.F. Gilmour, *Analysis of a nonlinear partial difference equation, and its application to cardiac dynamics*, J. Difference Equations and Appl., 8 (2002), pp.1147-1169.

[55] K.H.W.J. Ten Tusscher, O. Bernus, R. Hren and A.V. Panfilov, *Comparison of electrophysiological models for human ventricular cells and tissues*, Prog. Biophys. Molecular Biology, 90 (2006), pp.326-345.

[56] A. Vinet, *Quasiperiodic circus movement in a loop model of cardiac tissue: Multistability and low dimensional equivalence*, Ann. Biomed. Eng., 28 (2000), pp.704-720.

[57] M.A. Watanabe, F.H. Fenton, S.J. Evans, H.M. Hastings and A. Karma, *Mechanisms for discordant alternans*, J. Cardiovascular Electrophysiol., 12 (2001), pp.196-206.

[58] M.A. Watanabe and M.L. Koller, *Mathematical analysis of dynamics of cardiac memory and accommodation: Theory and experiment,* Am. J. Physiol., 282 (2002), pp.H1534-H1547.

[59] M.A. Wood, P.M. Simpson, B.S. Stambler, J.M. Herre, R.C. Bernstein and K.A. Ellenbogen, *Long-term temporal patterns of ventricular tachyarrhythmias*, Circulation, 91 (1995), pp.2371-2377.

[60] M.A. Wood, P.M. Simpson, W.B. London, B.S. Stambler, J.M. Herre, R.C. Bernstein, K.A. Ellenbogen, *Circadian patterns of ventricular tachycardia in patients with implantable cardioverter defibrillators*, J. Am. Coll. Cardiol., 25 (1995), pp.901-907.

[61] M.A. Wood, P.M. Simpson, L.S. Liebovitch, A.T. Todorov and K.A. Ellenbogen, *Temporal patterns of ventricular tachyarrhythmias: Insights from the implantable cardioverter-defibrillator*, in: S.B. Dunbar, K.A. Ellenbogen and A.E. Epstein (Ed.s), *Sudden Cardiac Death: Past, Present and Future*, Futura Pub. Co., Armonk, NY, 1997.